Sādhanā (2021)46:120
https://doi.org/10.1007/s12046-021-01645-w

Bio-sensing application of chalcogenide thin film in a graphene-based surface plasmon resonance (SPR) sensor

JITENDRA SINGH TAMANG[1,2,*], RUDRA SANKAR DHAR[1,*], AKASH KUMAR BHOI[3], ARUN KUMAR SINGH[2] and SOMENATH CHATTERJEE[4,*]

[1]Department of Electronics and Communication Engineering, National Institute of Technology, Mizoram, Chatlang, Aizwal 796 012, India
[2]Department of Electronics and Communication Engineering, Sikkim Manipal Institute of Technology (SMIT), Sikkim Manipal University (SMU), Majitar, Sikkim 737 136, India
[3]Department of Electrical and Electronics Engineering, Sikkim Manipal Institute of Technology (SMIT), Sikkim Manipal University (SMU), Majitar, Sikkim 737 136, India
[4]Centre for Material Science and Nano Technology, Sikkim Manipal Institute of Technology, Sikkim Manipal University, Majitar, Sikkim 737 136, India
e-mail: js.tamang@gmail.com; rdhar@uwaterloo.ca; somenath@gmail.com

MS received 14 January 2021; revised 13 April 2021; accepted 9 May 2021

Abstract. Chalcogenide Glasses are of recent interest in the field of chemical and bio-sensing applications. These are considered either in stored memory devices or in optical domain. The involvement of such material in the bio-sensing application for the development of SPR (Surface Plasmon Resonance) Sensors is very essential and thus, has been considered in this manuscript. In a Kretschmann SPR configuration, a thin-film layer of such Chalcogenide material has been incorporated which is further accompanied with a Graphene layer. The optical properties of both the materials viz. chalcogenide and graphene have been portrayed and presented in this paper by taking the assistance of MATLAB environment and Characteristic Transfer Matrix (CTM) Method.

Keywords. Chalcogenide glass; Surface plasmon resonance (SPR); Plasmonics; Kretschmann configuration; Graphene; Sensitivity; Signal-to-noise ratio (SNR).

1. Introduction

Surface Plasmon Resonance (SPR) has numerous applications viz. bio- and gas sensing [1] following the principle proposed as Drude Model [2] to know the nature of the plasmons involved in the SPR phenomenon. SPR considers different Kretschmann-Raether configurations [3] based on the kind of material and analyte to sense. SPR sensors should have huge possibility of increasing its sensitivity and selectivity property.

Chalcogens are chemical elements which although are toxic but are quite stable in nature. Chalcogenide materials uses such chalcogens in various sort of applications.

SPR sensor can also be developed based on a Chalcogenide material made of sulfide 2S2G and coated on a prism along with noble metal nanoparticles. The optical properties of such typical chalcogenide 2S2G material along with design parameters of the sensor further enhances the property of the SPR sensor in chemical and bio-chemical sensing considering the mechanism of angular interrogation [4]. SPR utilizes different form of glass-like Chalcogenide material (As-S-Se) as an active medium which reveals photoinduced changes and generates p and s-polarization. The thin film of the material had a higher sensitivity with a very high refractive index value which led it to find its utilization in memory and optical devices [5].

Chalcogenide material, too used in optic SPR sensor, can be developed including polymer and MoS2 in the clad region. The optic SPR sensor with the help of such material can discriminate a mixture of alcohols in a water solution. Apart from such chalcogenide materials, polythiophene films can also be used to increase the sensitivity property of a sensor and measure the optical fibre loss [6].

Graphene material can also be incoorporated in Chalcogenide (2S2G) based SPR prism along with gold material. The performance of such SPR sensor was examined and found to be better considering the properties of the chalcogenide and graphene material. With the help of these materials, the sensitivity and selectivity property was analysed and found to be more than the conventional SPR sensor [7].

Few Chalcogenide materials have a significant role in increasing the electrical properties as compared to other

*For correspondence
Published online: 16 June 2021

materials. It has been found that on making a small change in the concentration of any material in a heterogeneous mixture (considering chalcogen elements), not only the structural properties are changed, the energy levels as well as the characteristics are also affected [8]. In few cases, apart from using Au noble metal, a Chalcogenide SPR sensor can also be developed using Al active metal. With Al active metal, the parameters pertaining to SPR curve specially the sensitivity property was enhanced by more than 300%. In order to avoid Al to oxidise, Chalcogenide (2S2G) based SPR prism can be coated with a thin Au layer along with the Al metal [9]. Even the significance of Chalcogenide materials has been understood by following Admittance-Loci Method. The method provides a better selection and sensing property of the SPR sensor mostly in the infrared region irrespective of the type of sensing medium [10].

Optical fiber SPR sensors too, utilise the Chalcogenide materials for better and high-power electronic applications along with optical memory devices. Special sort of fibres so-called Holey fibres are incorporated with the chalcogenide glasses for generating single modes in the Fibre Optic SPR sensors taking small area of mode generation [11]. Chemical sensing is possible even by using other method apart from Characteristic Transfer Method (CTM). Different types of chemical samples viz. Carbon tetrachloride, Methyl salicylate, etc. are sensed and analysed using a basic SPR configuration and Admittance-Loci Method [12]. Polymer based Chalcogenide materials too have been employed in Fibre Optic SPR sensor.

Even 2D materials like graphene and inorganic compounds are utilised in infrared region in order to sense any analyte medium especially liver tissues perfectly [13]. The chalcogenide glasses find themselves very beneficial even in other applications apart from SPR sensors. The chalcogen material are highly important in the infrared region in order to detect negatively charged ions and electrons present in lung cells and thus finds application in biomedical field. The chalcogen materials, too are very useful in switching and generation of signals in infrared fibres [14]. Chalcogenide materials can also be helpful in developing waveguides which can sense chemical amorphous element and can determine its sensitivity property.

Through the property, it can be well understood that the developed chalcogenide-based waveguides are much more superior than the fibre optic SPR sensors [15]. When an SPR biosensor is developed using the chalcogenide materials, its potentiality increases in the transmission part applicable in the infrared region. Even the sulphide glass can be experimentally chosen along with the basic SPR configuration in order to understand the sensing mechanism [16].

Apart from bio-sensing and chemical sensing applications, chalcogenide glass material can also be beneficial for sensing gaseous substances. While sensing a gas analyte, alloy materials are utilised in order to test how sensor performs in respect to its sensitivity. Even while investigating, the design parameters viz. size and volume of the nanoparticle, and the wavelength of the input light are being taken into account [17]. With coated gold noble metal, Molybdenum disulfide (MoS2) nanosheets and chalcogen materials, even antibodies or proteins are sensed using fibre optic SPR sensor. This not only amplifies and stabilises the SPR signal but also increases the sensitivity property of the sensor. These properties assist the sensor to find application in biomedical field [18].

In this manuscript, different biological samples are tested and with respect to the SPR curves, the Reflectivity and SPR angles are measured. Along with the measurement, the implication of the graphene and chalcogenide material too are tested and stated.

2. Modelling methods

SPR Bio-sensor is configured keeping in mind the basic Kretschmann-Raether configuration. The configuration generally requires the coupling mechanism between the laser beam and the thickness of different layers. The eigen values of the layers and the optical properties of the graphene material have been considered providing equal priority to all the layers. Apart from the consideration of the eigen values, the thickness of each layer is taken approximately equal to 50 nm. In such configuration, a TMD ChG (Chalcogenide) film layer is sandwiched between a noble metal layer viz. Gold and a Graphene (L $\times$ 0.34 nm) layer considering the fact that ChG film are characterized by high transparency in infrared region and also have high refractive index. The ChG film too provides greater thermal stability. Gold provides better sensitivity property and governs the coupling mechanism between the entire system along with the incident laser beam. The Graphene layer also provides better sensitivity along with high absorption property which assists the SPR sensor to yield productive result. Different biological samples [19–21] are chosen in order to detect them very easily even if they are contaminated or mixed with other samples by this non-destructive, efficient and cost-effective technique.

Figure 1 shows the basic Multilayer SPR Kretschmann-Raether configuration comprising of Prism (SF10)/Metal (Gold)/ChG Film/N-Graphene layer (L $\times$ 0.34 nm) and Sensing Medium (Biological Samples).

Five-Layer SPR Sensor Configuration (Mathematical Approach):

The Five-Layer SPR Sensor considers the N-Plasmonic Matrix Method having the following characteristic equations:

Prism (SF10) layer,

$$q_{prism} = \frac{\cos\theta_{prism}}{n_{prism}} \tag{1}$$

Noble Metal (Gold, Ag) layer,

$$q_{metal} = \sqrt{\frac{\in_{metal} - n_{prism}^2 \sin^2 \theta_{prism}}{\in_{metal}}} \quad (2)$$

$$\beta_{metal} = \frac{2\pi}{\lambda} d_{metal} \sqrt{(\in_{metal} - n_{prism}^2 \sin^2 \theta_{prism})} \quad (3)$$

$$M_{metal} = \begin{bmatrix} \cos \beta_{metal} & -i \sin \beta_{metal}/q_{metal} \\ -q_{metal} \sin \beta_{metal} & \cos \beta_{metal} \end{bmatrix} \quad (4)$$

where M_{metal} is the characteristic matrix for Gold layer.

Chalcogenide (ChG) layer,

$$q_{ChG} = \frac{\sqrt{n_{ChG}^2 - n_{prism}^2 \sin^2 \theta_{prism}}}{n_{ChG}^2} \quad (5)$$

$$\beta_{ChG} = \frac{2\pi}{\lambda} d_{ChG} \sqrt{(n_{ChG}^2 - n_{prism}^2 \sin^2 \theta_{prism})} \quad (6)$$

$$M_{ChG} = \begin{bmatrix} \cos \beta_{ChG} & -i \sin \beta_{ChG}/q_{ChG} \\ -q_{ChG} \sin \beta_{ChG} & \cos \beta_{ChG} \end{bmatrix} \quad (7)$$

where M_{ChG} is the characteristic matrix for ChG layer.

N-Layer Graphene,

$$q_{graphene} = \frac{\sqrt{n_{graphene}^2 - n_{prism}^2 \sin^2 \theta_{prism}}}{n_{graphene}^2} \quad (8)$$

$$\beta_{graphene} = \frac{2\pi}{\lambda} d_{graphene} \sqrt{(n_{graphene}^2 - n_{prism}^2 \sin^2 \theta_{prism})} \quad (9)$$

$$M_{graphene} = \begin{bmatrix} \cos \beta_{graphene} & -i \sin \beta_{graphene}/q_{graphene} \\ -q_{graphene} \sin \beta_{graphene} & \cos \beta_{graphene} \end{bmatrix} \quad (10)$$

where $M_{graphene}$ is the characteristic matrix for N-Graphene layer.

$$M = M_{metal} * M_{ChG} = \begin{bmatrix} M_{11} & M_{12} \\ M_{21} & M_{22} \end{bmatrix} \quad (11)$$

where

$$M_{11} = \cos \beta_{metal} \cos \beta_{ChG} - \left(\frac{q_{ChG}}{q_{metal}}\right) \sin \beta_{metal} \beta_{ChG} \quad (12)$$

$$M_{12} = -i\left(\frac{\cos \beta_{metal} \sin \beta_{ChG}}{q_{ChG}} + \frac{\sin \beta_{metal} \cos \beta_{ChG}}{q_{metal}}\right) \quad (13)$$

$$M_{21} = (\cos \beta_{metal} \sin \beta_{ChG} q_{ChG} + \sin \beta_{metal} \cos \beta_{ChG} q_{metal}) \quad (14)$$

$$M_{22} = \cos \beta_{metal} \cos \beta_{ChG} - \left(\frac{q_{metal}}{q_{ChG}}\right) \sin \beta_{metal} \beta_{ChG} \quad (15)$$

Biological Sample layer,

$$q_{bio} = \frac{\sqrt{\left(n_{bio}^2 - n_{prism}^2 \sin^2 \theta_{prism}\right)}}{n_{bio}^2} \quad (16)$$

where q_{bio} is TM mode for Bio-Sample layer.

The reflectivity coefficient for TM mode is given by

$$r^p = \frac{\left((M_{11} + M_{12} q_{bio}) q_{prism} - (M_{21} + M_{22} q_{bio})\right)}{\left((M_{11} + M_{12} q_{bio}) q_{prism} + (M_{21} + M_{22} q_{bio})\right)} \quad (17)$$

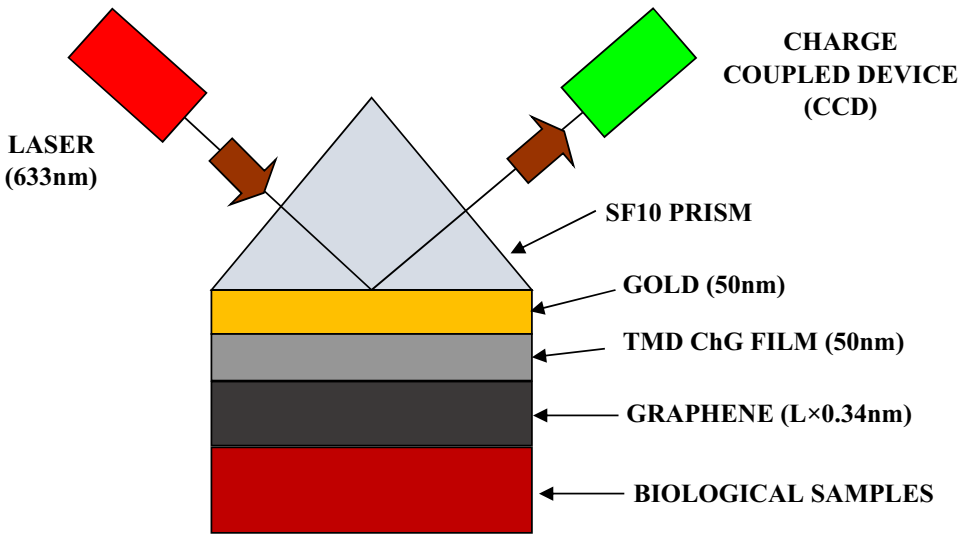

Figure 1. Schematic diagram of 5-layer Kretschmann–Raether configuration.

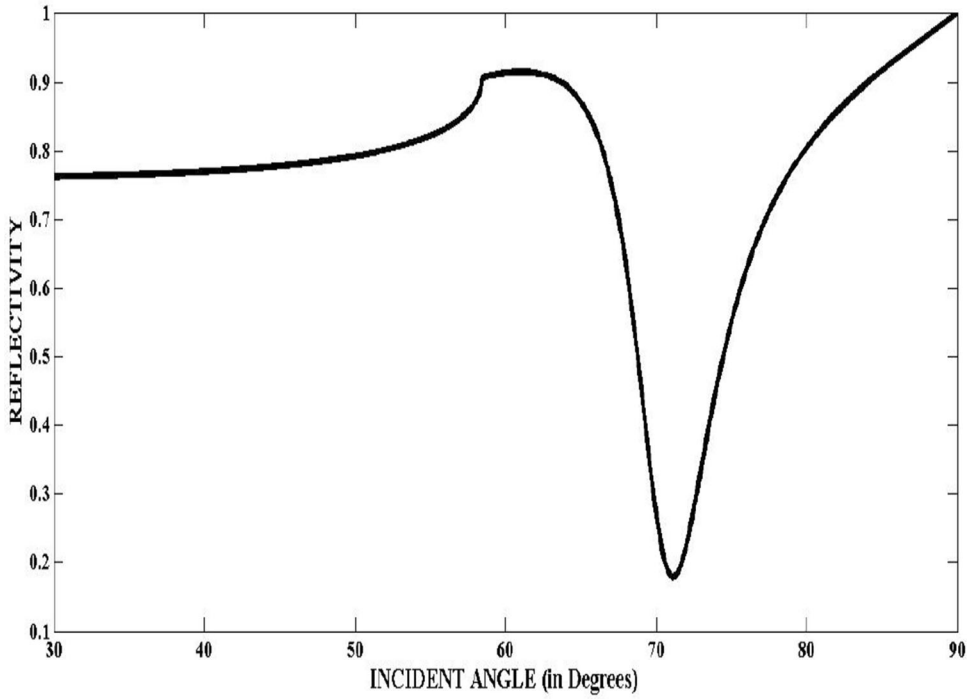

Figure 2. Reflectivity curve for SF10, ChG Thin Film Layer, Gold, Graphene-1 Layer and Cellulose.

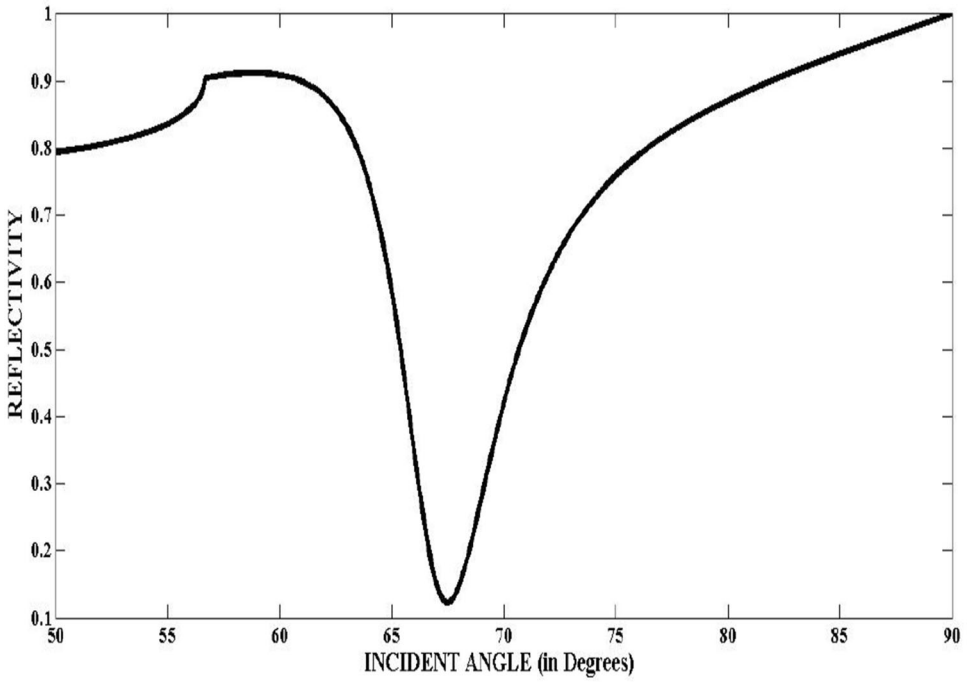

Figure 3. Reflectivity curve for SF10, ChG Thin Film Layer, Gold, Graphene-1 Layer and Glucose.

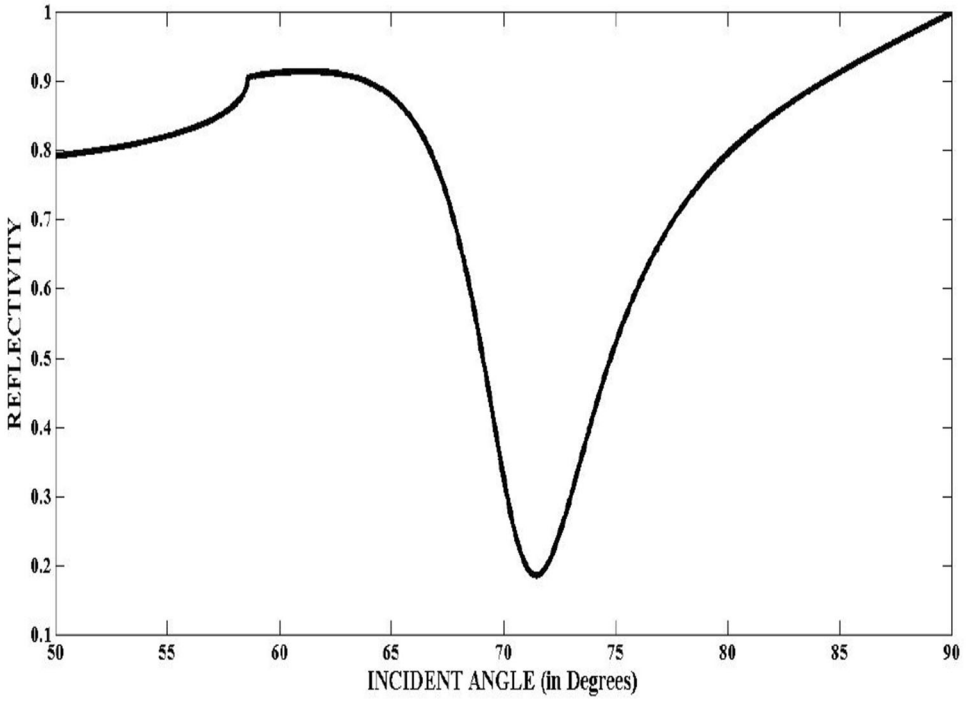

Figure 4. Reflectivity curve for SF10, ChG Thin Film Layer, Gold, Graphene-1 Layer and Glycerol.

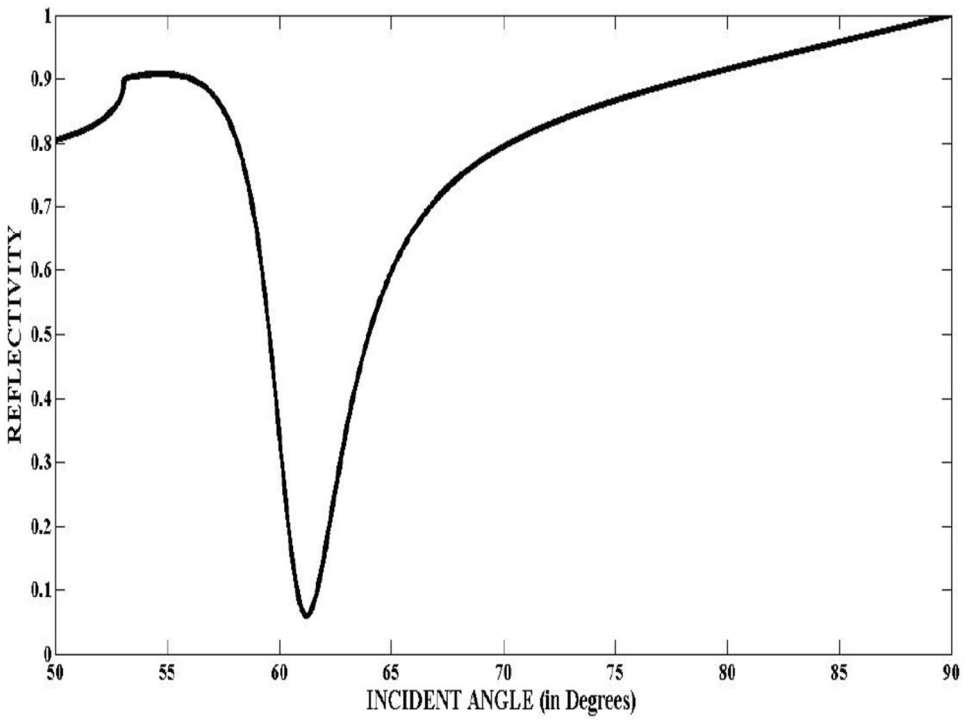

Figure 5. Reflectivity curve for SF10, ChG Thin Film Layer, Gold, Graphene-1 Layer and Isopropanol.

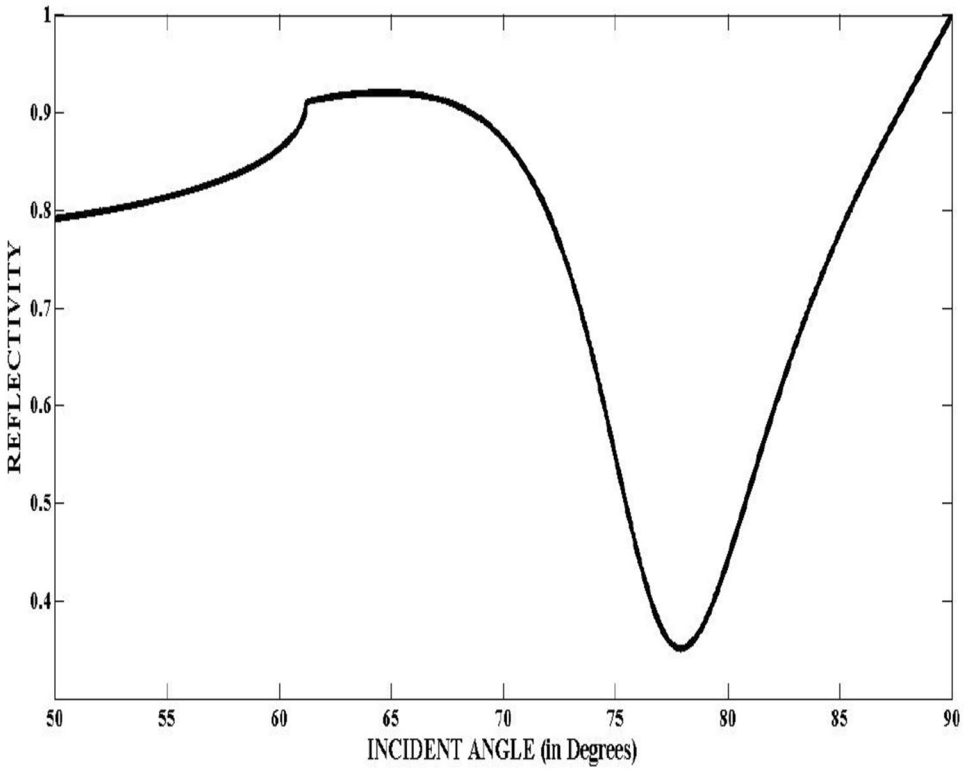

Figure 6. Reflectivity curve for SF10, ChG Thin Film Layer, Gold, Graphene-1 Layer and Polyaniline.

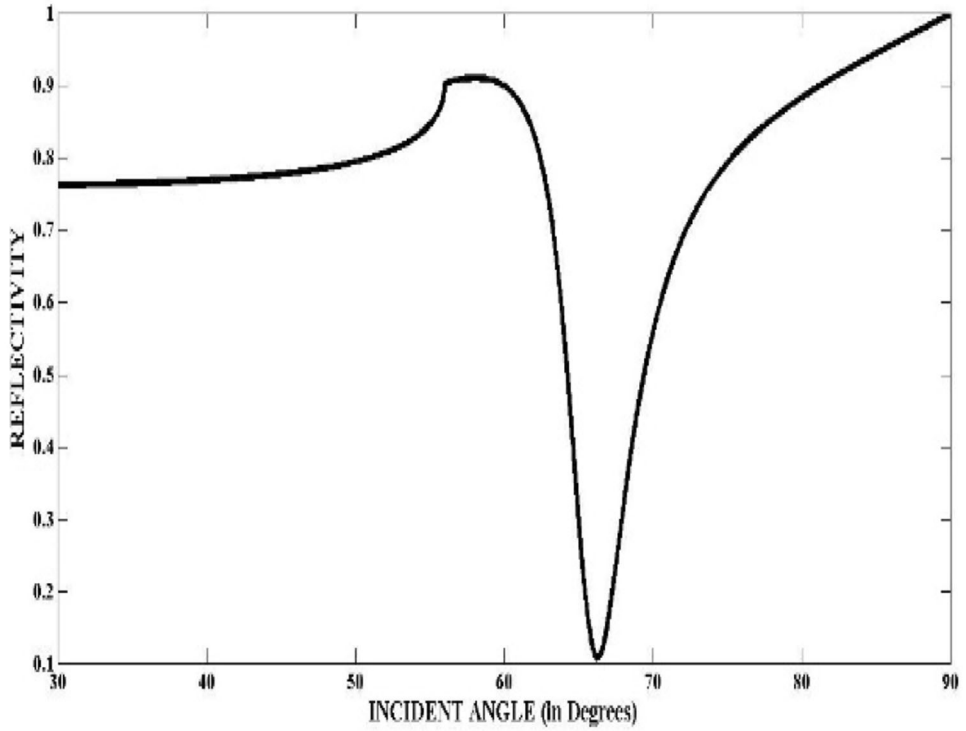

Figure 7. Reflectivity curve for SF10, ChG Thin Film Layer, Gold, Graphene-1 Layer and N,N-DIPA (Diisopropylaminoethanol).

Table 1. SPR Angle & Reflectivity Values of different Organic Samples considering SF10 as Prism.

Sl. No.	Biological Sample (Organic)	Reflectivity Value	SPR/Incident Angle (in Degrees)
1.	Cellulose	0.1787	71.09°
2.	Glucose	0.1223	67.46°
3.	Glycerol	0.1848	71.43°
4.	Isopropanol	0.0591	61.21°
5.	Polyaniline	0.3508	77.91°
6.	N,N-DIPA (Diisopropylaminoethanol)	1.4287	66.27°

The SPR curve can be obtained using the reflectivity equation which is given by

$$R = |r^p|^2 \tag{18}$$

3. Results and discussion

Figures 2, 3, 4, 5, 6 and 7 represent different biological samples as organic materials with respect to the Reflectivity (SPR) Curves. It can be clearly noticed that the detection of the organic material viz. Cellulose, Isopropanol, DIPA (Diisopropylamine) are easily possible as the width of the curve is narrower compared to the other organic materials. Even the reflectivity value of the DIPA (Diisopropylamine) is very less in comparison to other biological materials. Table 1 shows the complete Reflectivity and SPR/Incident Angle values.

Figures 8, 9, 10 and 11 characterize SPR curves of different biological (Human) samples as organic materials. In this case, detection of blood if mixed with any homogeneous solution can be easily identified as it has a very narrower curve width in comparison with other human biological samples. Table1 shows the complete Reflectivity and SPR/Incident Angle values.

4. Conclusion

Based on the SPR/Incident Angle values of Organic and Human Biological Samples, the shift in the angle depicts the characteristic of each sample. Organic samples can be detected easily as most of the samples fall under the range of 60°-75° and above while the Human Biological samples can be identified within the range of 55°-65°. However, the detection accuracy is maximum in case of DIPA (Diisopropylaminoethanol) and Blood Sample. DIPA is a colorless chemical liquid and extremely toxic. Thus, detection of such liquid results in avoiding any health hazardous.

Apart from detection, the reflectivity values of few biological samples are noted and found to be perfect

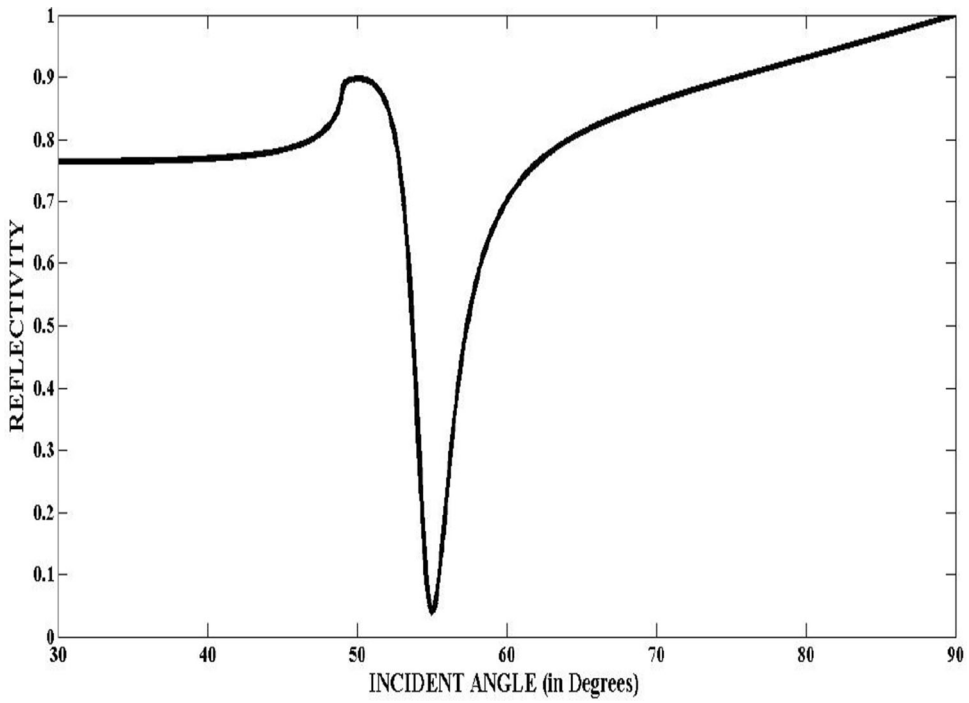

Figure 8. Reflectivity curve for SF10, ChG Thin Film Layer, Gold, Graphene-1 Layer and Blood Sample.

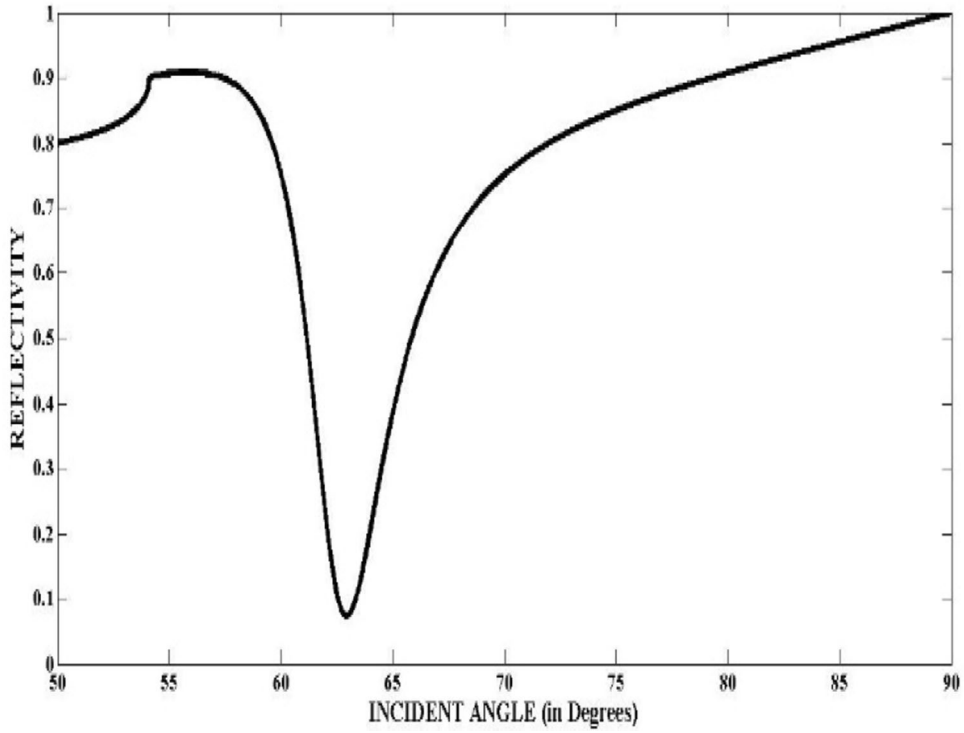

Figure 9. Reflectivity curve for SF10, ChG Thin Film Layer, Gold, Graphene-1 Layer and Eye Lens Sample.

for absorption process. Reflectivity values of Isopropanol, Blood Sample and Eye Lens Sample are very less approximately 0.05%. Less reflectivity value shows the property of Graphene material used in the modelling of SPR sensor. Thus, SPR sensor may be efficient both in terms of sensitivity and absorption even if biological (organic and human) samples are considered.

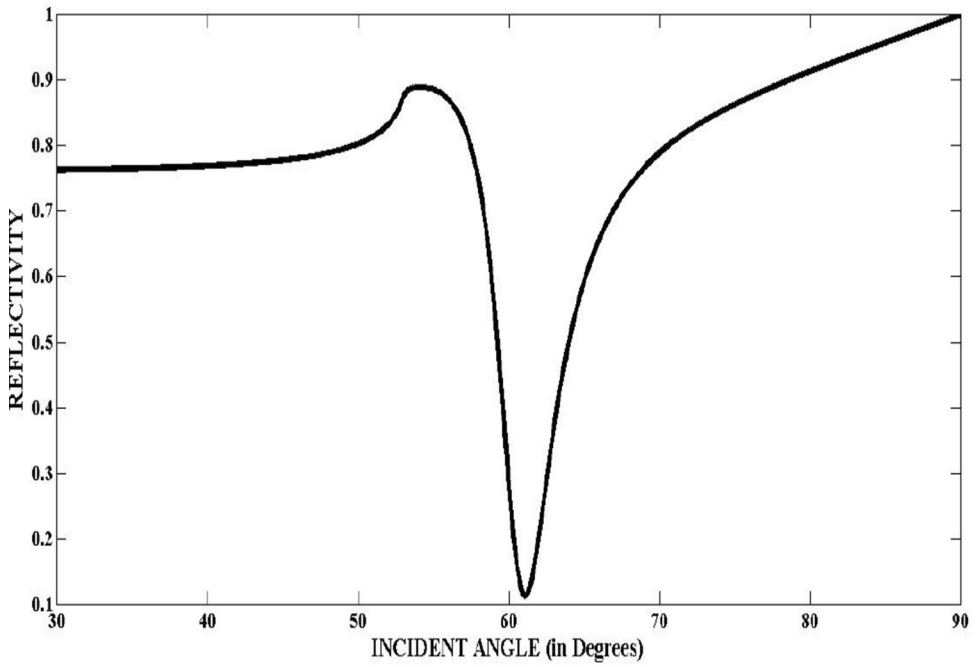

Figure 10. Reflectivity curve for SF10, ChG Thin Film Layer, Gold, Graphene-1 Layer and Liver Sample.

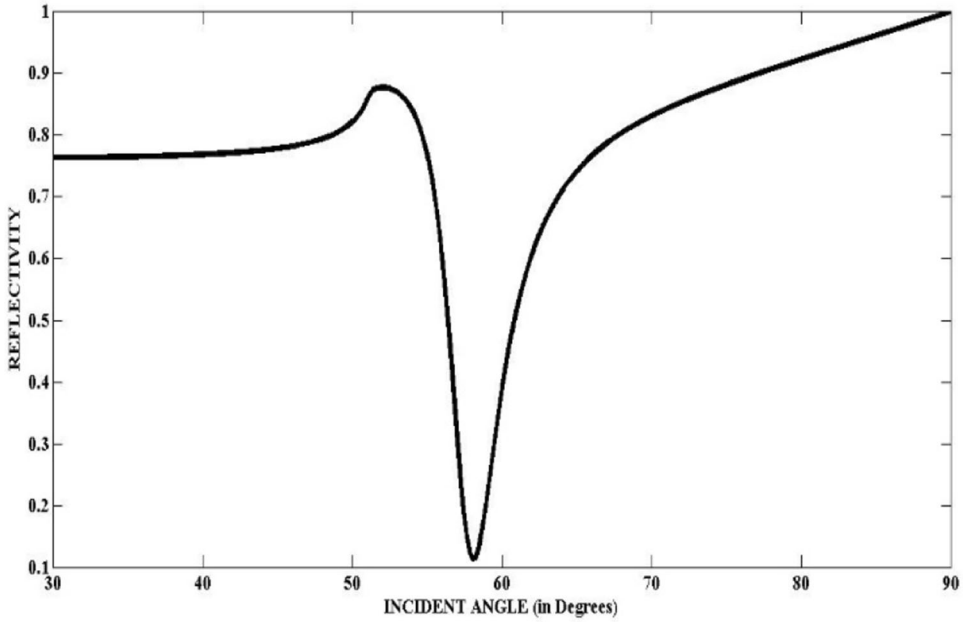

Figure 11. Reflectivity curve for SF10, ChG Thin Film Layer, Gold, Graphene-1 Layer and Colon (Mucosa) Sample.

Table 2. SPR Angle & Reflectivity Values of different Human Samples considering SF10 as Prism

Sl. No.	Biological Sample (Human)	Reflectivity Value	SPR/Incident Angle (in Degrees)
1.	Blood Sample	0.03826	55°
2.	Eye Lens Sample	0.07292	62.93°
3.	Liver Sample	0.1121	61.1°
4.	Colon (Mucosa) Sample	0.1131	58.1°

References

[1] Liedberg B, Nylander C and Lunström I 1983 Surface plasmon resonance for gas detection and biosensing. *Sens. Actuat.* 4: 299–304

[2] Paul D 1900 ZurElektronentheorie der metalle. *Ann. Phys.* 306(3): 566–613

[3] Kretchmann E and Rather H 1968 Radiative decay of non-radiative surface plasmons excited by light. *Naturforsch* 23: 2135–2136

[4] Jha R and Sharma A K 2009 Chalcogenide glass prism based SPR sensor with Ag–Au bimetallic nanoparticle alloy in infrared wavelength region. *J. Opt. A Pure Appl. Opt.* 11(4): 045502

[5] Popescu A A, Savastru R, Savastru D and Miclos S 2011 Application of vitreous As-S-Se chalcogenides as active layer in surface plasmon resonance configuration. *Dig. J. Nanomater. Biostruct.* 6(3): 1245–1252

[6] Sharma A K and Kaur B 2018 Chalcogenide fiber-optic SPR chemical sensor with MoS2 monolayer, polymer clad, and polythiophene layer in NIR using selective ray launching. *Opt. Fiber Technol.* 43: 163–168

[7] Maharana P K and Jha R 2012 Chalcogenide prism and graphene multilayer-based surface plasmon resonance affinity biosensor for high performance. *Sens. Actuat. B Chem.* 169: 161–166

[8] Singh A K 2014 Comparative study on structural and electrical properties of Se-Zn-In and Se-Zn-Te-in chalcogenide glasses. *Adv. Optoelectron. Mater.* 2: 1–10

[9] Jha R and Sharma A K 2009 High-performance sensor based on surface plasmon resonance with chalcogenide prism and aluminium for detection in infrared. *Opt. Lett.* 34(6): 749–751

[10] Brahmachari K and Ray M 2012 Influence of chalcogenide glass on surface plasmon resonance based sensor design in near infrared region using admittance loci method, In: *2012 5th International conference on computers and devices for communication (CODEC)*, IEEE, 1-4

[11] Person J L, Smektala F, Brilland C T L, Thierry J, Johann T and Dominique B 2006 Light guidance in new chalcogenide holey fibres from GeGaSbS glass. *Mater. Res. Bull.* 41(7): 1303–1309

[12] Brahmachari K and Ray M 2013 Modelling of chalcogenide glass based plasmonic structure for chemical sensing using near infrared light. *Optik* 124(21): 5170–5176

[13] Kaur B and Sharma A K 2018 Plasmonic biosensor in NIR with chalcogenide glass material: on the role of probe geometry, wavelength, and 2D Material. *Sens. Imaging* 19(1): 36

[14] Bruno B, Zhang X H, Smektala F, Jean-Luc A, Troles J, Ma H-L, Boussard-Ple'del C, Lucas J, Lucas P, Le Coq D, Riley M R, Simmons J H 2004 Recent advances in chalcogenide glasses. *J. Non-crystal. Solids* 345: 276–283

[15] Baschir L, Aurelian A P, Savastru D and Miclos S 2020 Surface plasmon resonance chemical sensors based on amorphous chalcogenide waveguides. *Macromol. Symp.* 389(1): 1900066

[16] Person L, Florent C J, Compere C, Lehaitre M, Anne M-L, Boussard-Plédel C, Bruno B, Adam J-L, Députier S and Guilloux-Viry M 2008 Surface plasmon resonance in chalcogenide glass-based optical system. *Sens. Actuat. B Chem.* 130(2): 771–776

[17] Sharma A K and Jha R 2009 Surface plasmon resonance-based gas sensor with chalcogenide glass and bimetallic alloy nanoparticle layer. *J. Appl. Phys.* 106(10): 103101

[18] Siddharth K, Tiwari U K, Deep A and Sinha R K 2019 Two-dimensional transition metal dichalcogenides assisted bio-functionalized optical fiber SPR biosensor for efficient and rapid detection of bovine serum albumin. *Sci. Rep.* 9(1): 1–11

[19] Matiatou M, Giannios P, Koutsoumpos S, Toutouzas K G, Zografos G C and Moutzouris K 2021 Data on the refractive index of freshly-excised human tissues in the visible and near-infrared spectral range. *Results Phys.* 22: 103833

[20] Giannios P, Koutsoumpos S, Toutouzas K G, Matiatou M, Zografos G C and Moutzouris K 2017 Complex refractive index of normal and malignant human colorectal tissue in the visible and near-infrared. *J. Biophoton.* 10(2): 303–310

[21] Myers T L, Tonkyn R G, Danby T O, Taubman M S, Bernacki B E, Birnbaum J C, Sharpe S W and Johnson T J 2018 Accurate measurement of the optical constants n and k for a series of 57 inorganic and organic liquids for optical modeling and detection. *Appl. Spectrosc* 72(4): 535–550